Main Manuscript for

Social Dominance Reorganizes the Transcriptomic Neuropeptidome in a Highly Social Cichlid Fish

Isaac Miller-Crews[1,†] and Hans A. Hofmann[1,2]

[1]Department of Integrative Biology, The University of Texas at Austin, Austin, TX

[2]Institute for Neuroscience, The University of Texas at Austin, Austin, TX

[†]Current address: Department of Biology, Indiana University, Bloomington, IN

* Isaac Miller-Crews and Hans A. Hofmann

Email: imillerc@iu.edu and hans@utexas.edu

Author Contributions: I.M-C and H.A.H. designed research; performed research; analyzed data; and wrote the paper.

Competing Interest Statement: Authors declare no competing interests.

Classification: Biological Sciences, Neuroscience

Keywords: Single-nucleus RNA-seq, neuropeptide networks, Hypothalamus, Preoptic area (POA), Social behavior

This PDF file includes:

Main Text
Figures 1 to 4

Abstract

Complex behavioral phenotypes, such as social status, emerge from the genome across biological levels, with many of the fundamental neural mechanisms shared across vertebrates. While various aspects of the brain have been implicated in modulating social behavior, critical regulators include cells of the preoptic area (POA) and hypothalamus, which by applying cellular-resolution transcriptomic approaches allows for greater exploration of cellular dynamics in these cells. Yet, how complex gene networks function between and within cell types to regulate complex social behavior is still poorly understood. Importantly, when considering functionally relevant neuronal classes of genes such as neuropeptides, understanding the inherent complexity that emerges from the interaction of these genes in the transcriptomic neuropeptidome can provide unique insight into how social behavior is regulated. Here, we used single-nucleus RNA-sequencing in the hypothalamus and POA of a highly social cichlid fish, *Astatotilapia burtoni*, to understand the effect that social status has on cellular-level transcriptomic profiles. Males of this species are well known for their highly plastic phenotypes related to social status, which allows for a hypothesis-driven approach. We demonstrate how social status manifests in changes of gene co-expression networks across neuronal populations and highlight transcriptomic signatures of social dominance when targeting known functional differences among AVP neuronal cell types. We implement a novel approach to relate how differences in social state translate to the integration of the transcriptomic neuropeptidome. Taken together, this research provides insights into how gene expression networks that modulate social behavior, including neuropeptide networks, function at the cellular level.

Significance Statement

Here, we used single-nucleus RNA-seq in the hypothalamus and POA of *Astatotilapia burtoni* to understand the effect that social status has on cellular gene expression. We demonstrate how social status manifests, from changes in broader neuronal gene networks to targeted changes between known socially-relevant neurons. For the first time, we assess the entirety of the transcriptomic neuropeptidome to understand the interaction of neuropeptide gene networks with social dominance. These findings provide a valuable resource for future functional work and an analytical framework for comparative studies on the evolution of the neural mechanisms of social behavior. Insights into the transcriptomic networks that modulate social status, specifically with neuropeptides, aid in our understanding of the complexity inherent in social behavior.

Main Text

Introduction

Many of the fundamental neural mechanisms that regulate social behavior are shared across vertebrates, due either to evolutionary conservation or to convergence (for review, see (1, 2)). Numerous brain regions and neuron populations associated with different aspects of social behavior have been identified by their activity patterns (e.g., immediate-early gene expression) and connectivity (e.g., tract tracing) (1, 3, 4). In recent years, open-ended genome-scale approaches, such as bulk or single-cell RNA-sequencing, have greatly expanded the scope of social neuroscience by uncovering the highly integrated and multifaceted nature of behavioral regulation by the brain (5–7). These advances also suggest an important and previously underappreciated role of glia cells in social behavior (8). However, how all these biological systems work together within and between specific cell types in relevant brain regions to encode and regulate complex social behavior is still poorly understood.

The hypothalamus and preoptic area (POA) are highly conserved brain regions across vertebrates (9) and serve as key neural nodes in regulating basic homeostatic processes such as energy balance, reproduction, stress physiology and many other functions (10–12), including

regulating social behavior (13, 14). The hypothalamus is a complex neural region, with multiple distinguishable subdivisions assigned by neuron morphology and function (15). In mammals, for example, the ventromedial hypothalamic nucleus (VMH) is well characterized for regulating aggression (16), while sex differences in the anteroventral periventricular nucleus (AVPV) can drive differences in parental behavior (17). Even though the homology relationships of these subdivisions across vertebrates are not always clear, studies in non-mammalian vertebrates suggest similar functions (18). Recent single-cell RNA-sequencing studies in mouse hypothalamus have demonstrated the cellular complexity of the region (19–21) and how its cellular inventory is likely driving the functional differences in other brain regions (22). Due to the high degree of cellular heterogeneity of functionally distinct neurons compared to other brain regions (e.g., hippocampus, neocortex, cerebellum, etc.), structure-function relationships are often difficult to establish in the hypothalamus and POA (20, 23).

As a consequence of both the structural and neuropeptide complexity of the hypothalamus and POA, a comprehensive and integrative understanding of the mechanisms through which this brain region regulates social behavior has been elusive. The situation is further complicated by the observation that the hypothalamus and POA is a major source of neuropeptides. In fact, neuropeptides and the neurosecretory cells that produce them date back to the ur-metazoan ancestor and possibly played a major role in the evolution of neurons (24, 25). Neuropeptides are enzymatically cleaved in the brain from larger precursor proteins (preprohormones) and often act as neuromodulators or neurohormones throughout the brain and, upon secretion from the brain, the entire organism (26, 27). Even small neuropeptides are known to coordinate a plethora of behavioral and physiological processes (28). In fact, numerous neuropeptide signaling pathways have been shown to regulate these homeostatic processes (e.g., energy balance: leptin, grehlin (29); reproduction: gonadotropin-releasing hormone (*GnRH 1*), gonadotropin-inhibiting hormone, kisspeptin (30); stress axis: corticotrophin-releasing factor (31); somatic growth: growth hormone (*GH*), somatostatin (*SST*) (32)). In mammals, over 130 peptide encoding genes have been identified, the vast majority of which are expressed in the hypothalamus and POA (33–35), and many also have important, evolutionarily conserved roles in regulating different aspects of social behavior (1). Because preprohormone genes usually encode at least two, and often more, neuropeptides, the resulting combinatorial complexity is staggering (27, 28, 36). Therefore, to understand the role that neuropeptides play in regulating social behavior the entirety of neuropeptide genes expression, the transcriptomic neuropeptidome, needs to be considered at the cellular level.

The role of the hypothalamus and POA in regulating social dominance has been examined in detail in Burton's Mouthbrooder cichlid, *Astatotilapia burtoni,* a highly social fish that has become an important model system in social neuroscience (37–39). Males of this species are characterized by plastic phenotypes associated with social dominance status with well-established differences in neural gene expression patterns and neuron morphology (for review, see (40)). Importantly, *A. burtoni* easily allows for consistent engineering of individuals in distinct social states that serve to represent both a phenotype and social role, which have critical consequences on health and fitness. There has been considerable research on the relationship of social status and peptidergic signaling in the hypothalamus and POA in *A. burtoni* (41, 42). For example, both *GnRH I* and *SST* expressing neurons are larger in size and have increased expression in dominant compared to subordinate males (32, 43). Likewise, three morphological subpopulations of vasopressin (AVP) neurons, parvo-, magno-, and giganto-cellular vary across social status of both males (44) and females (45). Specifically, gigantocelluar AVP neurons have higher AVP expression in dominant males while parvocellular AVP neurons show the opposite effect. Even though these cells are morphologically distinct, and appear to have unique responses to social status, it remains unknown what differences exist at other biological levels, such as the transcriptome. Several other neuropeptide systems have also been implicated in the regulation of social dominance in *A. burtoni* (for review see (37, 39)). To compare across these neuropeptide systems, O'Connell & Hofmann (46) integrated behavior, physiology, and bulk transcriptomics of the POA in dominant and subordinate *A. burtoni* males demonstrating that several key pathways may serve as conduits for social plasticity across multiple levels. This

suggests that environmentally induced changes at one level of biological organization do not simply affect changes of similar magnitude at other levels. However, previous studies lacked the cellular resolution that is necessary to match functionally important molecular pathways to specific cell types.

In the present study, we use snRNA-seq to analyze the hypothalamus and POA of dominant and subordinate *Astatotilapia burtoni* males. We investigated how differences in social status are linked to distinct transcriptomic profiles at the cellular level across three main hypotheses. First, we hypothesized that since genes function within the context of the transcriptome, neuronal gene co-expression networks are differentially regulated across social status and not just reflect neuronal cellular subtypes. Second, we hypothesized that morphologically distinct and socially responsive subpopulations of AVP neurons represent unique transcriptomic nuclei clusters that show differential expression patterns across social status at the subpopulation level rather than a ubiquitous change across all AVP expressing neurons. Third, given the role neuropeptides play in regulating behavioral changes, we sought to characterize the transcriptomic neuropeptidome at the cellular level to understand how the variation across social states will be reflected, hypothesizing that a more complex and overexpressed neuropeptidome would occur in dominant males.

Results

Cell type identification of sequenced hypothalamus nuclei.

We identified 27,870 individual single-cell transcriptomes across all samples and successfully demultiplexed three genotypes per sample pool between dominant and subordinate *A. burtoni* males (Fig. 1 A and B). Cell-type calling demonstrated consistency of cell types across social status and biological replicates (Fig. 1C) for six major hypothalamic neural cell categories: excitatory neurons (GLU), inhibitory neurons (GABA), oligodendrocytes, astrocytes, vascular cells, and cells of the *pars tuberalis* (21).

We then wanted to test whether there was any difference in the number of cell subtypes due to social status. We compared the proportion of nuclei clusters across social states with a binomial GLM (for detailed statistics see Dataset S1). Of all nuclei clusters, twelve appear to have biased proportion of nuclei from either dominant (6, 7, 12, 17, 20, 26, 27, 28) or subordinate males (2, 11, 16, 24) (Fig. 1D; Fig. S1). Three GLU nuclei clusters, clusters 11, 16, and 24 showed subordinate bias effect of at least 0.5, with GABA cluster 2 also having a subordinate bias. Of the eight clusters with a dominant bias, four are GLU (cluster 7, 12, 20, and 26), two are unknown (cluster 6 and 28), and two are oligodendrocytes (cluster 17 and 27).

For each of the non-neuron cell types (oligodendrocytes, astrocytes, vascular cells, and cells of the *pars tuberalis*), DEG analysis identified several significantly different genes across social status at the cell-type specific sub-cluster level (Fig. S2-S5). There is a total of 355 differentially expressed genes (FDR corrected p-value < 0.05) between social states across all four of the non-neuronal cell types. Of those, 29 genes are consistently and concordantly differentially expressed across all four non-neuronal cell types, including *gh1, prl, fshb, pomc, oxt, lhb* (Fig. S6). This result demonstrates that all cell types reflect social status to some extent and reveals a core set of differentially expressed genes across all cell types.

Neuron transcriptomic networks and social dominance

Subsequent hierarchical clustering of neurons demonstrated the presence of highly structured subpopulations, including excitatory and inhibitory neurons (Fig. 2A). We compared the proportion of neuron clusters across social states with a binomial GLM that included individual genotypes (for detailed statistics see Dataset S1). Of neuron clusters, twelve appear to have biased proportion of nuclei (FDR p-value < 0.01) either increased in dominant (3, 5, 7, 13, 14, and 16) or subordinate males (1, 6, 10, and 11) (Fig. 2B; Fig. S1C).

We then wanted to assess transcriptomic level responses to social status with gene co-expression networks. We analyzed neuron gene co-expression networks using hdWGCNA by generating metacell profiles separated by both social status and genotype. We found seven gene

co-expression modules across neurons (Fig. 2C). We found that gene modules complement UMAP clusters with some module eigengene expression levels being highly correlated with UMAP cluster (e.g. brown module) while others are more broadly represented across UMAP clusters (e.g. red module). Differential module eigengene expression analysis identified certain gene modules that are significantly differentially expressed across social status in both directions (Fig. 2D), with three modules significantly increased in dominant males (brown, red, and turquoise modules) and two modules significantly increased in subordinate males (blue and yellow modules), suggesting that the activity of certain gene networks is social status-dependent. We next used GO enrichment analysis to identify putative role of these modules (Dataset S2; Fig. S7). For example, the most differentially expressed dominant module, brown, has no functional enrichment. The most differentially expressed subordinate module, blue, is significantly enriched for cell-to-cell adhesion and neuron development.

Next, we wanted to compare the relationship between module eigengene expression for a given cluster and the degree of bias in nuclei counts across social states. For each neuron cluster, we calculated the average module eigengene value and assigned the module with the maximum eigengene value for that cluster as an indication which module has the strongest relationship to a neuron cluster. Of the neuron clusters with a significant social status bias in cell counts, most of those clusters were maximally related to modules with a significant increase in module eigengene for that status as well: dominant males [7-blue; 5,3-brown; 16-black; 14-turquoise; 13-red]; subordinate males [6,10,11-blue; 1-yellow] (neuron cluster-maximum module).

Neurons expressing arginine vasopressin (AVP) pre-prohormone mRNA

Previous research identified three preoptic AVP-positive neuron populations that varied in size (representing the parvo-, magno-, and gigantocellular portions of the POA, respectively) and were regulated differently by social status (44). To determine whether these three AVP neuron populations also emerge from our single cell data, we first identified all neurons that expressed AVP preprohormone mRNA, resulting in 254 and 236 nuclei for dominant and subordinate males, respectively. Hierarchical clustering of these AVP expressing neurons discerned five clusters that are present in all six genotypes (Fig. 3A). The average AVP expression level for each cluster per genotype was calculated and we found that AVP neuron cluster 4 had a higher average AVP expression compared to all other AVP neuron clusters (Fig. 3B). We then looked at immediate early gene (IEG) expression levels as a proxy for AVP neuron activity. We found that what appears to be differential expression of IEG across social status with an increase in dominant males in AVP neuron cluster 1 and an increase in subordinate males in AVP neuron cluster 4 (Fig. S8).

To assign AVP neuron clusters to potential brain regions, we used a spatial location prediction score (See Supplemental Materials) for the broader neuron clusters and assigned putative spatial location to AVP neuron clusters based on the broader neuron cluster that the majority of AVP neurons from each AVP neuron cluster was from. We were particularly interested in matching to one cluster from the HypoMap (21) dataset (C66-22: Caprin2.GLU-6) assigned to the paraventricular nucleus (PVN) that shows the highest amount of gene expression for both AVP and OXT (Fig. S9). We found the best match for this HypoMap cluster is AVP neuron cluster 1. Additionally, we predicted spatial location of AVP neuron cluster 1 as the mammalian paraventricular nucleus (PVN) and AVP neuron cluster 4 as the mammalian ventromedial hypothalamic nucleus (Fig. S9).

We then wanted to test if AVP neuron clusters had differentially expressed genes (DEGs) across social states. Differential gene expression for the 500 most variable genes across AVP neurons was performed with limmatrend, across genotypes, for all AVP neurons and each AVP cluster. We found that there were distinct socially regulated differentially expressed genes within each AVP neuron subpopulation (Fig. 3C). These subpopulation differences are obscured when comparing DEGs of all AVP neurons across social status. While there are some genes that appear to be consistently dominant biased across AVP neuron subpopulations (*prl, gh1, oxt, cga, MT: 1,086*), only a few genes are uniquely differentially expressed for a given AVP neuron subpopulation (AVP neuron cluster 0: *ND1, CYTB, MT: 70*; AVP neuron cluster 1: *COX*; AVP

neuron cluster 4: *col12a1b*). Likewise, there are no genes that are consistently higher in subordinates among AVP neuron subpopulations, with mores genes uniquely differentially expressed for a give AVP neuron subpopulation (AVP neuron cluster 0: *pcbp3, meis2a.1, Epha5*; AVP neuron cluster 1: *or106-8, TAFA5.1*; AVP neuron cluster 3: *mkxa, adamts6, vipr1b*; AVP neuron cluster 4: *si:ch211-13k12.2*).

Uncovering the transcriptomic neuropeptidome

To understand the role of neuropeptides, which have a known functional role in regulating social status, we were interested in the totality of interactions across all neuropeptides, the transcriptomic neuropeptidome. We aimed to uncover how cellular expression of neuropeptide networks differs across social status. First, neuropeptide preprohormone encoding genes were collated from a series of mammalian databases and orthologs determined for each. Then for each neuronal nuclei we counted the number of different neuropeptide genes expressed within each sample. For the 60 annotated neuropeptide preprohormones, we found that >99% of neurons express at least one neuropeptide. Next, we compared the distribution of neuropeptides per neuron across social status (Fig. 4A). We found that the distribution of the number of neuropeptides per neuron was from the same distribution across dominant males (AD = 1.013, p = 0.890), subordinate males (AD = 0.623, p = 0.996), and across all samples (AD = 1.970, p = 0.999). Similarly, we found no difference in the number of neuropeptides per neuron within dominant males (Poisson, β = -0.006 & 0.006, SE = 0.010 & 0.010, p = 0.565& 0.551) or within subordinate males (Poisson, β = -0.021 & -0.006, SE = 0.133 & 0.137, p = 0.133 & 0.646) indicating that the counts were consistent across individuals of the same social status. We found that dominant male neurons are expected to have a significant 33% increase in neuropeptide genes expressed compared to subordinate male neurons (Poisson, β = -0.414, SE = 0.007, p < 2e-16).

We next compared the number of neurons expressing each neuropeptide across social status to find neuropeptides that are more broadly expressed in one social state over the other (Fig. 4B). We found that 23/60 neuropeptides were significantly different (FDR pvalue <0.05) between dominant and subordinate males in the number of neuronal nuclei those neuropeptide genes are expressed (for detailed stats on binomial GLM results see Dataset S1). There are 3 genes with a subordinate bias (*cort, NPFF, gnrh3*) and 20 with a dominant bias (*agrp, vip, hcrt, iapp, NPY, npy, kiss2, penk, gal, SST, pomc, vgf, NMB, scg5, nxph1, adcyap1b, GNRH1, scg2b, prl, oxt*).

Since neuropeptide gene co-expression was so widespread, we then quantified the difference across the transcriptomic neuropeptidome between social states. First, we wanted to test that the relationship of the transcriptomic neuropeptidome between dominant and subordinate males. Comparing the average neuropeptide co-expression network across genotypes of dominants and subordinates found that these networks are significantly positively correlated (Mantel test: r = 0.18, 95% CI for r = 0.07-0.25; p = 0.003), indicating that the overall pattern of the networks is not different. Next, we wanted to test if the networks were significantly different, even if the overall pattern was similar. We used two methods to test for equality of the two high-dimensional covariance matrices from these networks that both found a significant (p-value < 0.001) difference: HD statistic of ~55 (47) and CLX statistic of ~2998 (48). Therefore, these methods indicate that the neuropeptide gene co-expression networks are correlated but have significant differences between social states.

We wanted to determine which pairs of neuropeptide genes differ in their co-expression across social status. We used the neuropeptide gene co-expression networks to find the difference between dominant and subordinate individuals for each pair of neuropeptide genes (Fig. 4C; Fig. S10). We found that almost all neuropeptides display a significant increase (FDR adjusted p-value < 0.05) in relative neuropeptide co-expression in dominant males, except for the significantly higher co-expression in subordinate males between: *cort* and *CHGA*; *cort* and *scg2b*. Next, we tested whether neuropeptide co-expression networks differed in how closely clustered they are between social states by measuring transitivity overall (Fig. 4D). Global transitivity of the neuropeptide gene co-expression networks indicates that dominant males

(global transitivity = 0.853) have a higher probability of shared connections among nodes than subordinate males (global transitivity = 0.748). Likewise, we used local transitivity of each neuropeptide gene within the network to quantify how connected the neighbors of that gene are to each other. Similar to the global transitivity results, more neuropeptide genes have higher local transitivity in the dominant network. This indicates that genes in dominant male neuropeptidome tend to cluster together more relative to subordinate male, an indicator of increased gene co-expression network connectivity. Of note, the dominant biased neuropeptide genes (*gnrh1, prl, pomc*) had almost no transitivity in subordinate networks. The presence of dominant biased neuropeptide genes with high degrees of local transitivity highlights how dominant males not only have neurons uniquely expressing these genes but that these genes therefore have status-specific neuropeptide co-expression networks.

Discussion

In the present study, we examined how social status is reflected in the variation of cell type-specific transcriptomic profiles across the hypothalamus and POA. We successfully implemented single-nucleus RNA-seq in a non-traditional model organism to identify the transcriptomic changes associated with social dominance in the hypothalamus and POA of males in *A. burtoni* (Fig. 1). We observed notable changes across social status in the expression of gene co-expression networks within neurons. Our approach was able to target specific known functional neural populations of AVP neurons to assess the impact of the social environment on gene expression. We applied a novel framework for understanding the role the entire transcriptomic neuropeptidome plays in social status. Taken together, we show how multiple biological systems integrate at the transcriptomic level as part of the signature of social role in the brain; status is important for the organization of social animals as a key driver of health and fitness.

Neural transcriptome dynamics across and within cell types

We demonstrate how cell types beyond neurons appear to be impacted to some degree by social status, as a common core set of 29 genes are significantly differentiated across non-neuronal cell types (Fig. S6). In fact, 12 of the 33 cell types have a significant bias between social states in the relative proportion of nuclei, with two of those cell types being oligodendrocytes with a dominant male bias (Fig. 1D). This aligns with previous work on the role of non-neuronal cell types in regulating social behavior (8). Oligodendrocyte cellular gene-expression appears to be particularly sensitive to environmental stimuli, such as previously shown with fasting in mouse hindbrain (49) and hypothalamus (50). There has also been extensive work studying the role of oligodendrocytes in response to social isolation across various brain regions, although less so in the hypothalamus (for review, see (51)).This remains an exciting line for future research into how non-neuronal cell types regulate social behavior, especially in brain regions such as the hypothalamus in which much of the work has traditionally focused on peptidergic neurons.

In the present study, we primarily focused on the gene networks occurring within neurons due to their direct functional role in regulating brain activity and social behavior, and as neurons are known to exhibit a relatively high degree of transcriptomic variability and subpopulation structure (20). Using a specialized gene co-expression network approach, hdWGCNA (52), we were able to characterize gene networks that go beyond neuronal cell-type or statistical cluster (Fig. 2). One assumption that is commonly made about gene networks derived from WGCNA-type approaches in bulk RNA-seq data is that these gene modules reflect cellular-level transcriptomes, hence why those genes are correlated in the first place. As such, we predicted that there would be more modules within a neuron sub-type with only a few broader modules representing gene pathways involved in ubiquitous cell function, and therefore, unlikely to be related to social dominance. Therefore, we were surprised to find that only the brown module appears to be mainly restricted to one of the broad neuronal cell types within inhibitory neurons. This implies that most gene co-expression networks do not necessarily represent major cell-type stratification, but are rather tied into cell state, function, and likely spatial distribution.

Yet, we found that both the broader and more cell-type restricted modules could be differentially expressed across social status, and based on the GO analysis, the strongest differentially expressed module across social status, blue module, is significantly enriched for interactions between cells and neuron development (Dataset S2; Fig. S7A). This could indicate that the underlying differences in neurons driving regulation of social status are integral to the development and interaction between neurons. Spatial transcriptomics could provide future insights into relating neuron cellular-level transcriptome dynamics with neuron spatial distribution and neural wiring.

Vasopressin neuronal subpopulations in relation to social dominance

The vasopressin system has long been studied for its role in regulating social behavior (53). We find evidence that there are multiple subpopulations of *AVP* expressing neurons based on the cellular-level transcriptome (Fig. 3). This is consistent with morphological and spatial data identifying multiple subpopulations of *AVP* expressing neurons (18, 45, 54, 55), although we discovered five distinct molecular cell types of *AVP* expressing neurons, indicating that untangling the relationship within these subpopulations will require further study. We did identify that *AVP* neuron cluster 4 had the highest *AVP* expression and would therefore be a likely candidate to represent parvocellular neurons, which are also known to have the highest *AVP* expression levels (44). Yet, using the HypoMap (21) database as a reference, we predicted the spatial assignment of *AVP* neuron cluster 4 to regions outside of the POA in the VMH, which would likely be similar to *AVP* subpopulations previously identified in putative teleost homolog (ATN) (45, 56) (Fig. S9C). Meanwhile, *AVP* neuron cluster 1 was spatially assigned to the mammalian paraventricular nucleus, which is the putative homolog of the parvocellular cells in the teleost POA (18, 55). While by no means a comprehensive assessment, this reinforces that the statistical clusters found in single-cell data can indeed reflect the cell types found through other neuroscientific approaches and could be expanded towards the study of other candidate genes.

Previous research in *A. burtoni* demonstrated that the three main morphological subpopulations of AVP neurons – parvo-, magno-, and giganto-cellular – have distinct *AVP* expression patterns across social states (44, 45). Importantly, these status dependent expression levels are masked when looking at bulk expression of the POA or hypothalamus (44, 46, 57) Additionally, *AVP*, and not *OXT*, has been shown to have a status dependent role in male social dominance across specific regions of the POA in other species such as the weakly electric fish (58). Surprisingly, we did not find any neuronal *AVP* subpopulations that showed differences in *AVP* expression level across social status (Fig. 1B). We did find some evidence that different subpopulations may exhibit different activity patterns across social status (Fig. S8D). Previous work in *A. burtoni* has demonstrated higher *egr-1* expression following aggressive behavior in AVP magnocellular neurons (59). Therefore, the higher *egr-1* expression we found occurring in AVP cluster 1 of dominant males could be related to the increased aggression seen in these males and potentially indicates that these AVP neurons are in fact AVP magnocellular neurons. While this study was not designed to test neural activity patterns directly, these differences likely reflect ongoing differences in neuronal activity related to the vastly divergent behavioral repertories associated with social status and would require further study to verify. While there do appear to be a handful of genes that increased with social dominance, when analyzed separately, each of the neuronal *AVP* subpopulations showed a minor number of distinct differentially expressed genes (Fig. 3C). Importantly, analysis of all *AVP* expressing neurons together would have masked many of the genes that showed increased expression in subordinate males. This demonstrates that expression of one or a few genes does not fully define a cell, and the need to consider the entirety of the transcriptome within that cell.

Immunohistochemical studies of AVP and OXT peptidergic neurons have long suggested that these two nonapeptides show little to no co-colocalization (60). In contrast, our study found remarkable co-expression of both AVP and OXT preprohormone mRNA across cell types (Fig. S8). In *A. burtoni* the OXT system has not been studied to the same degree as AVP (61, 62) (but see: (63)), yet similar to *AVP*, past work has found no status difference of *OXT* expression when using data bulk POA data (46). While other studies have also showed that *OXT* is broadly

375 expressed (64), peptide studies indicate that only a subset of cells in the POA contain the OXT
376 peptide in fish (65–67). Although our findings are not entirely unprecedented as small populations
377 of neurons co-expressing *AVP* and *OXT* have previously been shown in rats, specifically in
378 magnocellular neurons (68–71). In mammals, the co-expression of *AVP* and *OXT* could be
379 related to the close chromosomally orientation and proximity (only 3-11 kb apart), with the
380 intervening region known to regulate magnocellular specific expression patterns (72). Previous
381 work demonstrated the regulatory elements driving this cell-specific expression are conserved
382 from pufferfish using transgenic rats, even though in pufferfish there is greater physical
383 separation of these genes (46 kb apart with five intervening genes) and a reversal of orientation
384 (73). Since the *AVP* and *OXT* genes represent the preprohormones (see below), it is important to
385 consider that post-transcriptional processing produces the two neurophysin co-peptides that
386 facilitate the neurosecretory granule packaging and transport of *AVP* and *OXT* prohormone via
387 axons, thereby protecting these neuropeptides from degradation (26, 74–77). Yet, these
388 neurophysins do not appear to co-localize with their opposite neuropeptide counterpart (78),
389 indicating again that *AVP* and *OXT* preprohormones may have co-localized transcription but are
390 less likely to have co-localized translation. While in rodents it appears that some post-
391 transcriptional process largely prevents the co-expression and co-localization of AVP and OXT,
392 more research is needed to understand whether this functional separation is maintained across
393 vertebrates and how it is reconciled with the prevalent co-expression of *AVP* and *OXT*
394 preprohormone mRNA in this teleost system.
395
396 *Uncovering the Transcriptomic Neuropeptidome*
397 The presence of neuropeptides and neurosecretory cells date back to metazoan
398 ancestors and likely drive the evolution of neurons (24, 25). Prior to single-cell transcriptomic
399 approaches, cellular-level resolution of neuropeptide expression has been limited to a single
400 gene, or at most a couple of genes, making wide-scale co-expression analysis difficult (79).
401 Previous single-cell RNA-seq experiments in mouse hypothalamus demonstrated how 27
402 neuropeptide genes are limited to a few neuronal subtypes, but co-expression of multiple
403 neuropeptides is common in hypothalamic neurons, with some being broadly expressed across
404 subtypes and others more specific (similar pattern found in neuropeptide receptors) (80). With our
405 approach to demultiplexing into genotypes, we demonstrate the consistency of these co-
406 expression networks across individuals and how neuropeptide co-expression depends on social
407 status (Fig. 4).
408 Importantly, expression of a preprohormone does not necessarily lead to mature peptides
409 or guarantee secretion (81). While trying to understand the impact of the transcriptomic
410 neuropeptidome, we must recognize that gene expression levels represent preprohormone
411 mRNA, not mature peptide levels. Starting with the discovery that the POMC gene could produce
412 multiple peptides (82–85), it became apparent that preprohormones generally encode two or
413 more peptides, which may or may not all be produced (27, 28, 36). snRNA-seq only allows us to
414 estimate preprocessed nuclear mRNA of preprohormones and thus we cannot know which
415 specific, or combination of, peptide hormones is ultimately processed and secreted. For example,
416 previous work has demonstrated in *A. burtoni* a dominant-bias in peptide levels of GnRH1 (43)
417 and SST (32), only *GnRH1* preprohormone mRNA levels reflect this difference at the cellular
418 level. The mechanisms that maintain and regulate peptide translation therefore add an additional
419 layer of complexity to the neuropeptidome.
420 Finally, we found that 23/60 neuropeptide genes showed a significant difference in the
421 number of expressing cells across social status, with 20 being more broadly expressed in
422 dominant males and three in subordinate males (Fig. 4B). This confirms previous research
423 showing dominant males have elevated levels of *pomc* and *GnRH1* in the whole-brain
424 transcriptomes (57) and *SST* (32, 86). Dominant males not only have more neurons expressing
425 these neuropeptides but also have more highly integrated neuropeptide co-expression network
426 (Fig. 4C). In fact, this elevated gene network integration pattern in dominant male *A. burtoni* has
427 previously been demonstrated with a few select neuropeptides (46, 87). The combinatorial nature
428 of these cellular-level neuropeptide gene networks, taken together with this more integrated

network, implies that social status reflects more than simply the activation of a few well-studied gene pathways but a complex interplay across the genome.

Materials and Methods

Animals

The animals used in this study came from a laboratory population of Burton's Mouthbrooder cichlid, *Astatotilapia burtoni*, descended for about 60 generations from a wild-caught stock of 400 individuals (88). All work was done in compliance with the Institutional Animal Care and Use Committee (IACUC) at The University of Texas at Austin.

Experimental design

We created naturalistic laboratory communities of adult *A. burtoni*, with two males and three females each, to generate three pairs of dominant and subordinate males used to compare snRNA-seq of the hypothalamus and POA across social status (Fig. 1A). Detailed experimental methods are described in the Supplemental Materials.

Processing of single nucleus data

We obtained 926 million reads total (dominant samples pool: 460 million reads; subordinate samples pool: 466 million reads). We used the MultiQC package (89) to confirm that all reads had Phred scores above 35 and passed all quality control measures. Read mapping and annotation were implemented using the Cell Ranger 6.1.2 pipeline (90) and the Nile tilapia, *Oreochromis niloticus*, reference genome (O_niloticus_UMD_NMBU) (91). Data was then processed with the Seurat integrated analysis pipeline (92) and normalized with SCTransform version 2 (93). The cell by gene expression matrices for each pooled sample dataset were filtered by selecting genes expressed in a minimum of 3 cells and selecting nuclei with 1000-2000 detected genes (nFeature_RNA). This threshold was determined from the distribution of nuclei to reduce background and reduce doublets. We then clustered the nuclei using the standard Seurat pipeline, we utilized Clustree (94) to determine an appropriate resolution for clustering by selecting a resolution that yielded the most stable number of clusters (0.8). This resulted in a total of 15,392 and 12,514 single-nucleus transcriptomes for the dominant and subordinate sample pool respectively.

Genotype demultiplexing

Even though our *A. burtoni* laboratory population is not fully outbred (95, 96), we expected there to be sufficient genotypic variation to allow demultiplexing of pooled samples by genotype, thereby recovering biological replication for downstream statistical analyses. The inclusion of greater biological variation with identification of multiple individuals can further reduce any batch effects, although the main source would likely be due to sequencing and prep which were done at the same time. Genotypic variation in our *A. burtoni* populations allowed for demultiplexing of the pooled samples using genotype of each sample. We used the souporcell package (97) for this purpose, as it does not require the genotype of each individual in a pooled samples to be known. Briefly, the pipeline performs variant detection on the sequence bam files to count allele support for each nucleus. Next, the nuclei are clustered with a sparse mixture model to assign cells to genotypes. Together, this allows for demultiplexing in the absence of prior genotype information of each sample.

Cell type calling

We successfully recovered all major cell types previously identified in the hypothalamus (See Supplemental Materials). Importantly, this approach allowed us to reduce noise by characterizing nuclei with unknown cell types that did not get assigned to any specific cell category. The proportion of cell subtypes across social status was compared with a binomial GLM for each cell subtype separately (98) and FDR corrected to account for comparisons across all subtypes tested. To assign putative spatial location to neuron clusters in *A. burtoni*, we developed

483 a method for comparing these clusters to mouse hypothalamus neuron clusters with known or
484 imputed spatial information on the HypoMap database (21) (See Supplemental Materials).
485
486 *Differential gene expression analysis and weighted gene co-expression network analysis*
487 We further subclustered each cell type, mediating identification of subtypes, using UMAP
488 and Clustree (94) to determine the appropriate number of sub-clusters. Next, we used limmatrend
489 (99, 100), incorporating the genotype data to separate out pooled samples and add statistical
490 power, to identify differentially expressed genes (DEGs) across social status for each subtype
491 and across all nuclei of each cell type.
492 Nuclei identified as GABAergic "inhibitory" (GABA) and glutamatergic "excitatory" (GLU)
493 were merged into the broader neuron category. Due to the higher degree of complexity of
494 neurons, indicated by the presence of multiple sub-clusters, these neuron nuclei were
495 subsequently subset out of the dataset and re-clustered with UMAP into various sub-populations
496 of neurons. The proportion of neuron subtypes across social status was compared with a
497 binomial GLM for each cell subtype separately (98) and FDR corrected to account for
498 comparisons across all subtypes tested. Next, we performed a Weighted Gene Co-expression
499 Network Analysis (WGCNA) approach adapted for single-nucleus data, hdWGCNA (52), to
500 identify gene co-expression modules. Compared to traditional WGCNA (101), hdWGCNA was
501 developed specifically for use with single-cell and spatial transcriptomics data by generating
502 metacells from selected pools of nuclei to reduce background noise of typically noisy single-
503 nucleus transcriptomes. These metacells represent localized groups of cells distinct from seurat
504 clustering, using a K-nearest neighbors (KNN) algorithm, producing an expression matrix that has
505 less sparsity and, therefore, more amenable to correlation network approaches. Metacells were
506 pooled from individual samples using the genotyping data and with a minimum cell count
507 parameter of 50. We used limmatrend (99, 100) to identify differentially expressed genes (DEGs)
508 and differentially expressed module eigengenes (deMEGs) for these neuron populations between
509 dominant and subordinate groups using individual genotypes. Next, we asked if modules were
510 functionally enriched for specific gene ontology (GO) terms. We used AnnotationForge to
511 generate a GO database for Nile Tilapia (102), calculated GO enrichment with enrichGO from the
512 package clusterprofiler (103), with FDR corrected adjusted p-value cutoff of 0.15, minGSSize =
513 10, and maxGSSize = 500, and graphed our results the package enrichplot (104).
514
515 *Neuropeptide preprohormone co-expression networks*
516 To infer the structure of the transcriptomic neuropeptidome, the entirety of neuropeptide
517 genes expression within a cell, we collated known "neuropeptide genes" (encoding pre-
518 prohormone mRNAs) from several databases (33–35) and via Ensembl (105), resulting in 127
519 genes (Dataset S3). Presence/absence matrices of dominant and subordinate animals, with a
520 threshold of two reads, were constructed. We then wanted to compare if the number of neuronal
521 nuclei that expressed different numbers of neuropeptides came from the same distribution within
522 and across status with an Anderson-Darling k-Sample Test (106). To test if the distributions of
523 neuropeptide genes per neuronal nuclei differed across and within social status we used Poisson
524 regression. The proportion of neuronal nuclei expressing each neuropeptide genes across social
525 status was compared with a binomial GLM for each neuropeptide separately (98) and adjusted for
526 multiple comparisons within subtypes with a multivariate t distribution with the R package 'glht'
527 and adjusted again with FDR to account for comparisons across all subtypes tested. Due to the
528 higher total number of nuclei sequenced in dominant males, the number of neurons expressing
529 individual neuropeptide genes was calculated and scaled by ~60% for dominant males, the ratio
530 of dominant neuron counts to subordinate neuron counts. The correlation between the two
531 matrices was calculated with a mantel test. Equality of the two covariance matrices across social
532 status was tested with two methods developed specifically for high dimensional data using HD
533 (47), which is designed for large covariance matrices, and CLX (48), which is for testing sparse
534 but large magnitude differences. Next, we generated co-expression network of just neuropeptide
535 genes for each genotype, filtering out low expressing nuclei and genes. For each edge,
536 representing a neuropeptide gene pair, an FDR corrected t-test was used to determine if the

specific co-expression pair was dominant and subordinate biased. Global and local clustering coefficients were calculated with transitivity in igraph (107).

Data availability

The filtered deduplicated reads have been deposited to the NCBI Short Read Archive (SRA), bioproject PRJNA1310498. The code used in this paper together with documentation can be accessed as the GitHub repository, https://github.com/imillercrews/BurtoniSnRNAseq.

Acknowledgments

We thank Dr. Nihal A. Salem for guidance and the members of the Hofmann Lab for discussion and Holly Stevenson for technical assistance. We also thank Dr. Zackary V. Johnson and Dr. Tessa K. Solomon-Lane for helpful suggestions and feedback on the manuscript. Sequencing was performed by the Genomic Sequencing and Analysis Facility at UT Austin, Center for Biomedical Research Support (RRID# SCR_021713). Computational analyses were performed using the Biomedical Research Computing Facility at UT Austin, Center for Biomedical Research Support (RRID#: SCR_021979). This work was supported by a US Department of Justice graduate fellowship, a UT Austin Graduate School Summer Fellowship, an IB graduate research grant, and Blair Scholarship fund in Zoology to IMC and NSF-IOS grant 1354942 and the William H. and Gladys G. Reeder Fellowship to HAH. IMC currently funded by Common Themes in Reproductive Diversity NIH 2T32HD049336.

References

1. L. A. O'Connell, H. A. Hofmann, Evolution of a Vertebrate Social Decision-Making Network. *Science* **336**, 1154–1157 (2012).

2. C. C. Rittschof, G. E. Robinson, "Chapter Five - Behavioral Genetic Toolkits: Toward the Evolutionary Origins of Complex Phenotypes" in *Current Topics in Developmental Biology*, Genes and Evolution., V. Orgogozo, Ed. (Academic Press, 2016), pp. 157–204.

3. J. L. Goodson, The vertebrate social behavior network: Evolutionary themes and variations. *Horm. Behav.* **48**, 11–22 (2005).

4. S. W. Newman, The Medial Extended Amygdala in Male Reproductive Behavior A Node in the Mammalian Social Behavior Network. *Ann. N. Y. Acad. Sci.* **877**, 242–257 (1999).

5. J. Chen, P. R. Richardson, C. Kirby, S. R. Eddy, H. E. Hoekstra, Cellular evolution of the hypothalamic preoptic area of behaviorally divergent deer mice. *eLife* **13**, RP103109 (2025).

6. E. K. Fischer, M. E. Hauber, A. M. Bell, Back to the basics? Transcriptomics offers integrative insights into the role of space, time and the environment for gene expression and behaviour. *Biol. Lett.* **17**, 20210293 (2021).

7. R. M. Harris, H. A. Hofmann, Neurogenomics of Behavioral Plasticity. *Adv. Exp. Med. Biol.* 149–168 (2013).

8. Z. V. Johnson, *et al.*, Cellular profiling of a recently-evolved social behavior in cichlid fishes. *Nat. Commun.* **14**, 4891 (2023).

579 9. S. A. Sower, M. Freamat, S. I. Kavanaugh, The origins of the vertebrate hypothalamic–
580 pituitary–gonadal (HPG) and hypothalamic–pituitary–thyroid (HPT) endocrine systems:
581 New insights from lampreys. *Gen. Comp. Endocrinol.* **161**, 20–29 (2009).

582 10. H. Fong, J. Zheng, D. Kurrasch, The structural and functional complexity of the integrative
583 hypothalamus. *Science* **382**, 388–394 (2023).

584 11. C. B. Saper, B. B. Lowell, The hypothalamus. *Curr. Biol.* **24**, R1111–R1116 (2014).

585 12. Y. Xie, R. I. Dorsky, Development of the hypothalamus: conservation, modification and
586 innovation. *Development* **144**, 1588–1599 (2017).

587 13. J. Dominguez, E. Hull, Dopamine, the medial preoptic area, and male sexual behavior.
588 *Physiol. Behav.* **86**, 356–368 (2005).

589 14. L. A. Lemaire, C. Cao, P. H. Yoon, J. Long, M. Levine, The hypothalamus predates the origin
590 of vertebrates. *Sci. Adv.* **7**, eabf7452 (2021).

591 15. M. Benevento, T. Hökfelt, T. Harkany, Ontogenetic rules for the molecular diversification of
592 hypothalamic neurons. *Nat. Rev. Neurosci.* **23**, 611–627 (2022).

593 16. P. Chen, W. Hong, Neural Circuit Mechanisms of Social Behavior. *Neuron* **98**, 16–30 (2018).

594 17. N. Scott, M. Prigge, O. Yizhar, T. Kimchi, A sexually dimorphic hypothalamic circuit controls
595 maternal care and oxytocin secretion. *Nature* **525**, 519–522 (2015).

596 18. L. A. O'Connell, H. A. Hofmann, The Vertebrate mesolimbic reward system and social
597 behavior network: A comparative synthesis. *J. Comp. Neurol.* **519**, 3599–3639 (2011).

598 19. D. W. Kim, *et al.*, The cellular and molecular landscape of hypothalamic patterning and
599 differentiation from embryonic to late postnatal development. *Nat. Commun.* **11**, 4360
600 (2020).

601 20. R. A. Romanov, *et al.*, Molecular interrogation of hypothalamic organization reveals
602 distinct dopamine neuronal subtypes. *Nat. Neurosci.* **20**, 176–188 (2017).

603 21. L. Steuernagel, *et al.*, HypoMap—a unified single-cell gene expression atlas of the murine
604 hypothalamus. *Nat. Metab. 2022 410* **4**, 1402–1419 (2022).

605 22. Z. Zeng, N. Miao, T. Sun, Revealing cellular and molecular complexity of the central
606 nervous system using single cell sequencing. *Stem Cell Res. Ther.* **9**, 234 (2018).

607 23. H. S. Kaplan, *et al.*, Sensory input, sex and function shape hypothalamic cell type
608 development. *Nature* 1–12 (2025). https://doi.org/10.1038/s41586-025-08603-0.

609 24. E. Hayakawa, *et al.*, Mass spectrometry of short peptides reveals common features of
610 metazoan peptidergic neurons. *Nat. Ecol. Evol.* **6**, 1438–1448 (2022).

611 25. K. Tessmar-Raible, *et al.*, Conserved Sensory-Neurosecretory Cell Types in Annelid and Fish
612 Forebrain: Insights into Hypothalamus Evolution. *Cell* **129**, 1389–1400 (2007).

613 26. D. G. Bichet, "Chapter 8 - The Posterior Pituitary" in *The Pituitary (Third Edition)*, S.
614 Melmed, Ed. (Academic Press, 2011), pp. 261–299.

615 27. A. L. Wiggenhorn, *et al.*, A class of secreted mammalian peptides with potential to expand
616 cell-cell communication. *Nat. Commun.* **14**, 8125 (2023).

617 28. S. J. Smith, *et al.*, Single-cell transcriptomic evidence for dense intracortical neuropeptide
618 networks. *eLife* **8** (2019).

619 29. A. Sahu, Leptin signaling in the hypothalamus: emphasis on energy homeostasis and leptin
620 resistance. *Front. Neuroendocrinol.* **24**, 225–253 (2003).

621 30. L. J. Kriegsfeld, Driving reproduction: RFamide peptides behind the wheel. *Horm. Behav.*
622 **50**, 655–666 (2006).

623 31. N. Dedic, A. Chen, J. M. Deussing, The CRF Family of Neuropeptides and their Receptors -
624 Mediators of the Central Stress Response. *Curr. Mol. Pharmacol.* **11**, 4–31 (2018).

625 32. H. A. Hofmann, R. D. Fernald, Social status controls somatostatin neuron size and growth.
626 *J. Neurosci. Off. J. Soc. Neurosci.* **20**, 4740–4 (2000).

627 33. J. P. H. Burbach, Neuropeptides from concept to online database www.neuropeptides.nl.
628 *Eur. J. Pharmacol.* **626**, 27–48 (2010).

629 34. Y. Kim, S. Bark, V. Hook, N. Bandeira, NeuroPedia: neuropeptide database and spectral
630 library. *Bioinformatics* **27**, 2772–2773 (2011).

631 35. R. L. Seal, *et al.*, Genenames.org: the HGNC resources in 2023. *Nucleic Acids Res.* **51**,
632 D1003–D1009 (2023).

633 36. J. Douglass, O. Civelli, E. Herbert, Polyprotein gene expression: generation of diversity of
634 neuroendocrine peptides. *Annu. Rev. Biochem.* **53**, 665–715 (1984).

635 37. H. A. Hofmann, Gonadotropin-releasing hormone signaling in behavioral plasticity. *Curr.*
636 *Opin. Neurobiol.* **16**, 343–350 (2006).

637 38. H. A. Hofmann, R. D. Fernald, What cichlids tell us about the social regulation of brain and
638 behaviour. *J. Aquac. Aquat. Sci.* **9**, 17–31 (2001).

639 39. K. P. Maruska, R. D. Fernald, Astatotilapia burtoni: A Model System for Analyzing the
640 Neurobiology of Behavior. *ACS Chem. Neurosci.* **9**, 1951–1962 (2018).

641 40. K. P. Maruska, R. D. Fernald, Social Regulation of Male Reproductive Plasticity in an African
642 Cichlid Fish. *Integr. Comp. Biol.* **53**, 938–950 (2013).

643 41. J. M. Butler, E. M. Herath, A. Rimal, S. M. Whitlow, K. P. Maruska, Galanin neuron
644 activation in feeding, parental care, and infanticide in a mouthbrooding African cichlid fish.
645 *Horm. Behav.* **126**, 104870 (2020).

646 42. D. T. Porter, D. A. Roberts, K. P. Maruska, Distribution and female reproductive state
647 differences in orexigenic and anorexigenic neurons in the brain of the mouth brooding
648 African cichlid fish, Astatotilapia burtoni. *J. Comp. Neurol.* 1–32 (2017).
649 https://doi.org/10.1002/cne.24268.

650 43. M. R. Davis, R. D. Fernald, Social control of neuronal soma size. *J. Neurobiol.* **21**, 1180–
651 1188 (1990).

652 44. A. K. Greenwood, A. R. Wark, R. D. Fernald, H. A. Hofmann, Expression of arginine
653 vasotocin in distinct preoptic regions is associated with dominant and subordinate
654 behaviour in an African cichlid fish. *Proc. R. Soc. Lond. B Biol. Sci.* **275**, 2393–2402 (2008).

655 45. J. M. Butler, C. M. Anselmo, K. P. Maruska, Female Reproductive State is Associated with
656 Changes in Distinct Arginine Vasotocin Cell Types in the Preoptic Area of Astatotilapia
657 burtoni. *J. Comp. Neurol.* cne.24995 (2020). https://doi.org/10.1002/cne.24995.

658 46. L. A. O'Connell, H. A. Hofmann, Social status predicts how sex steroid receptors regulate
659 complex behavior across levels of biological organization. *Endocrinology* **153**, 1341–1351
660 (2012).

661 47. J. Chang, W. Zhou, W.-X. Zhou, L. Wang, Comparing large covariance matrices under weak
662 conditions on the dependence structure and its application to gene clustering. *Biometrics*
663 **73**, 31–41 (2017).

664 48. T. Cai, W. Liu, Y. Xia, Two-Sample Covariance Matrix Testing and Support Recovery in High-
665 Dimensional and Sparse Settings. *J. Am. Stat. Assoc.* **108**, 265–277 (2013).

666 49. G. K. C. Dowsett, *et al.*, A survey of the mouse hindbrain in the fed and fasted states using
667 single-nucleus RNA sequencing. *Mol. Metab.* **53**, 101240 (2021).

668 50. S. Kohnke, *et al.*, Nutritional regulation of oligodendrocyte differentiation regulates
669 perineuronal net remodeling in the median eminence. *Cell Rep.* **36**, 109362 (2021).

670 51. L. Tomlinson, C. V. Leiton, H. Colognato, Behavioral experiences as drivers of
671 oligodendrocyte lineage dynamics and myelin plasticity. *Neuropharmacology* **110**, 548–562
672 (2016).

673 52. S. Morabito, F. Reese, N. Rahimzadeh, E. Miyoshi, V. Swarup, hdWGCNA identifies co-
674 expression networks in high-dimensional transcriptomics data. *Cell Rep. Methods* **3**,
675 100498 (2023).

676 53. H. E. Albers, Species, Sex and Individual Differences in the Vasotocin/Vasopressin System:
677 Relationship to Neurochemical Signaling in the Social Behavior Neural Network. *Front.*
678 *Neuroendocrinol.* **0**, 49–71 (2015).

679 54. M. J. Braford, R. G. Northcutt, Organization of the diencephalon and pretectum of the ray-
680 finned fishes. *Fish Neurobiol.* **2**, 117–163 (1983).

681 55. F. L. Moore, C. A. Lowry, Comparative neuroanatomy of vasotocin and vasopressin in
682 amphibians and other vertebrates. *Comp. Biochem. Physiol. C Pharmacol. Toxicol.*
683 *Endocrinol.* **119**, 251–260 (1998).

684 56. J. L. Goodson, A. H. Bass, Vasotocin innervation and modulation of vocal-acoustic circuitry
685 in the teleost Porichthys notatus. *J. Comp. Neurol.* **422**, 363–379 (2000).

686 57. S. C. P. Renn, N. Aubin-Horth, H. A. Hofmann, Fish and chips: functional genomics of social
687 plasticity in an African cichlid fish. *J. Exp. Biol.* **211**, 3041–3056 (2008).

688 58. P. Pouso, Á. Cabana, V. Francia, A. Silva, Vasotocin but not isotocin is involved in the
689 emergence of the dominant-subordinate status in males of the weakly electric fish,
690 Gymnotus omarorum. *Horm. Behav.* **158**, 105446 (2024).

691 59. J. L. Loveland, R. D. Fernald, Differential activation of vasotocin neurons in contexts that
692 elicit aggression and courtship. *Behav. Brain Res.* **317**, 188–203 (2017).

693 60. M. Otero-García, C. Agustín-Pavón, E. Lanuza, F. Martínez-García, Distribution of oxytocin
694 and co-localization with arginine vasopressin in the brain of mice. *Brain Struct. Funct.* **221**,
695 3445–3473 (2016).

696 61. L. S. Huffman, *et al.*, Distribution of nonapeptide systems in the forebrain of an African
697 cichlid fish, Astatotilapia burtoni. *J. Chem. Neuroanat.* **44**, 86–97 (2012).

698 62. M. Rodriguez-Santiago, J. Nguyen, L. S. Winton, C. A. Weitekamp, H. A. Hofmann, Arginine
699 Vasotocin Preprohormone Is Expressed in Surprising Regions of the Teleost Forebrain.
700 *Front. Endocrinol.* **8** (2017).

701 63. C. A. Weitekamp, *et al.*, A Role for Oxytocin-Like Receptor in Social Habituation in a
702 Teleost. *Brain. Behav. Evol.* **89**, 153–161 (2017).

703 64. D. S. Quintana, *et al.*, Oxytocin pathway gene networks in the human brain. *Nat. Commun.*
704 **10**, 668 (2019).

705 65. T. F. C. Batten, M. L. Cambre, L. Moons, F. Vandesande, Comparative distribution of
706 neuropeptide-immunoreactive systems in the brain of the green molly, Poecilia latipinna.
707 *J. Comp. Neurol.* **302**, 893–919 (1990).

708 66. B. I. Holmqvist, P. Ekström, Galanin-like immunoreactivity in the brain of teleosts:
709 Distribution and relation to substance P, vasotocin, and isotocin in the atlantic salmon
710 (Salmo salar). *J. Comp. Neurol.* **306**, 361–381 (1991).

711 67. H. M. van den Dungen, R. M. Buijs, C. W. Pool, M. Terlou, The distribution of vasotocin and
712 isotocin in the brain of the rainbow trout. *J. Comp. Neurol.* **212**, 146–157 (1982).

713 68. E. Glasgow, *et al.*, Single Cell Reverse Transcription-Polymerase Chain Reaction Analysis of
714 Rat Supraoptic Magnocellular Neurons: Neuropeptide Phenotypes and High Voltage-Gated
715 Calcium Channel Subtypes. *Endocrinology* **140**, 5391–5401 (1999).

716 69. H. Kiyama, P. C. Emson, Evidence for the co-expression of oxytocin and vasopressin
717 messenger ribonucleic acids in magnocellular neurosecretory cells: simultaneous
718 demonstration of two neurohypophysin messenger ribonucleic acids by hybridization
719 histochemistry. *J. Neuroendocrinol.* **2**, 257–259 (1990).

720 70. D. Xi, K. Kusano, H. Gainer, Quantitative Analysis of Oxytocin and Vasopressin Messenger
721 Ribonucleic Acids in Single Magnocellular Neurons Isolated from Supraoptic Nucleus of Rat
722 Hypothalamus. *Endocrinology* **140**, 4677–4682 (1999).

723 71. E. Mezey, J. Z. Kiss, Coexpression of vasopressin and oxytocin in hypothalamic supraoptic
724 neurons of lactating rats. *Endocrinology* **129**, 1814–1820 (1991).

725 72. J. P. H. Burbach, S. M. Luckman, D. Murphy, H. Gainer, Gene Regulation in the
726 Magnocellular Hypothalamo-Neurohypophysial System. *Physiol. Rev.* **81**, 1197–1267
727 (2001).

728 73. B. Venkatesh, S. L. Si-Hoe, D. Murphy, S. Brenner, Transgenic rats reveal functional
729 conservation of regulatory controls between the Fugu isotocin and rat oxytocin genes.
730 *Proc. Natl. Acad. Sci. U. S. A.* **94**, 12462–12466 (1997).

731 74. H. B. V. Dyke, B. F. Chow, R. O. Greep, A. Rothen, The isolation of a protein from the par
732 neuralis of the ox pituitary with constant oxytocici, pressor and diuresis-inhibiting
733 activities. *J. Pharmacol. Exp. Ther.* **74**, 190–209 (1942).

734 75. D. B. Hope, M. Wälti, D. J. Winzor, Co-operative binding of oxytocin to bovine neurophysin
735 II. *Biochem. J.* **147**, 377–379 (1975).

736 76. P. Lin, A. Adem, D. Murphy, M. Greenwood, "How Does the Camel Survive in the Desert
737 Without Drinking?" in *Evolutionary and Comparative Neuroendocrinology*, V. Grinevich, R.
738 Oliveira, Eds. (Springer Nature Switzerland, 2025), pp. 389–423.

739 77. V. Pliška, H. Sachs, The Interaction of Lysine Vasopressin with Free and Agarose-Bound
740 Bovine Neurophysin II. *Eur. J. Biochem.* **41**, 229–239 (1974).

741 78. S. J. Watson, *et al.*, Immunocytochemistry of the C-terminal peptide of propressophysin
742 (CPP): Relationship to vasopressin, oxytocin and neurophysin. *Neuropeptides* **3**, 321–336
743 (1983).

744 79. K. H. Chen, A. N. Boettiger, J. R. Moffitt, S. Wang, X. Zhuang, Spatially resolved, highly
745 multiplexed RNA profiling in single cells. *Science* **348**, aaa6090 (2015).

746 80. R. Chen, X. Wu, L. Jiang, Y. Zhang, Single-Cell RNA-Seq Reveals Hypothalamic Cell Diversity.
747 *Cell Rep.* **18**, 3227–3241 (2017).

748 81. F. Meissner, R. A. Scheltema, H. J. Mollenkopf, M. Mann, Direct proteomic quantification
749 of the secretome of activated immune cells. *Science* **340**, 475–478 (2013).

750 82. R. E. Mains, B. A. Eipper, Biosynthesis of adrenocorticotropic hormone in mouse pituitary
751 tumor cells. *J. Biol. Chem.* **251**, 4115–4120 (1976).

752 83. R. E. Mains, B. A. Eipper, N. Ling, Common precursor to corticotropins and endorphins.
753 *Proc. Natl. Acad. Sci. U. S. A.* **74**, 3014–3018 (1977).

754 84. J. L. Roberts, E. Herbert, Characterization of a common precursor to corticotropin and
755 beta-lipotropin: identification of beta-lipotropin peptides and their arrangement relative
756 to corticotropin in the precursor synthesized in a cell-free system. *Proc. Natl. Acad. Sci. U.*
757 *S. A.* **74**, 5300–5304 (1977).

758 85. J. L. Roberts, E. Herbert, Characterization of a common precursor to corticotropin and
759 beta-lipotropin: cell-free synthesis of the precursor and identification of corticotropin
760 peptides in the molecule. *Proc. Natl. Acad. Sci. U. S. A.* **74**, 4826–4830 (1977).

761 86. B. C. Trainor, H. A. Hofmann, Somatostatin Regulates aggressive behavior in an african
762 cichlid fish. *Endocrinology* **147**, 5119–5125 (2006).

763 87. T. K. Solomon-Lane, H. A. Hofmann, Early-life social environment alters juvenile behavior
764 and neuroendocrine function in a highly social cichlid fish. *Horm. Behav.* **115**, 104552
765 (2019).

766 88. R. D. Fernald, N. R. Hirata, Field study of Haplochromis burtoni: Quantitative behavioural
767 observations. *Anim. Behav.* **25**, 964–975 (1977).

768 89. P. Ewels, M. Magnusson, S. Lundin, M. Käller, MultiQC: summarize analysis results for
769 multiple tools and samples in a single report. *Bioinformatics* **32**, 3047–3048 (2016).

770 90. G. X. Y. Zheng, *et al.*, Massively parallel digital transcriptional profiling of single cells. *Nat.*
771 *Commun.* **8**, 14049 (2017).

772 91. M. A. Conte, W. J. Gammerdinger, K. L. Bartie, D. J. Penman, T. D. Kocher, A high quality
773 assembly of the Nile Tilapia (Oreochromis niloticus) genome reveals the structure of two
774 sex determination regions. *BMC Genomics* **18**, 341 (2017).

775 92. R. Satija, J. A. Farrell, D. Gennert, A. F. Schier, A. Regev, Spatial reconstruction of single-cell
776 gene expression data. *Nat. Biotechnol.* **33**, 495–502 (2015).

777 93. S. Choudhary, R. Satija, Comparison and evaluation of statistical error models for scRNA-
778 seq. *Genome Biol.* **23**, 27 (2022).

779 94. L. Zappia, A. Oshlack, Clustering trees: a visualization for evaluating clusterings at multiple
780 resolutions. *GigaScience* **7**, giy083 (2018).

781 95. D. Brawand, *et al.*, The genomic substrate for adaptive radiation in African cichlid fish.
782 *Nature* **513**, 375–381 (2014).

783 96. I. Miller-Crews, M. V. Matz, H. A. Hofmann, A 2b-RAD parentage analysis pipeline for
784 complex and mixed DNA samples. *Forensic Sci. Int. Genet.* **55** (2021).

785 97. H. Heaton, *et al.*, Souporcell: robust clustering of single-cell RNA-seq data by genotype
786 without reference genotypes. *Nat. Methods 2020 176* **17**, 615–620 (2020).

787 98. L. E. Fuess, D. I. Bolnick, Single-Cell RNA Sequencing Reveals Microevolution of the
788 Stickleback Immune System. *Genome Biol. Evol.* **15**, evad053 (2023).

789 99. C. W. Law, Y. Chen, W. Shi, G. K. Smyth, voom: precision weights unlock linear model
790 analysis tools for RNA-seq read counts. *Genome Biol.* **15**, R29 (2014).

791 100. C. Soneson, M. D. Robinson, Bias, robustness and scalability in single-cell differential
792 expression analysis. *Nat. Methods 2018 154* **15**, 255–261 (2018).

793 101. P. Langfelder, S. Horvath, WGCNA: an R package for weighted correlation network analysis.
794 *BMC Bioinformatics* **9**, 559 (2008).

795 102. Carlson, M, Pagès, H, AnnotationForge: Tools for building SQLite-based annotation data
796 packages. (2024).

797 103. T. Wu, *et al.*, clusterProfiler 4.0: A universal enrichment tool for interpreting omics data.
798 *The Innovation* **2**, 100141 (2021).

799 104. Yu G, enrichplot: Visualization of Functional Enrichment Result. (2025).

800 105. F. J. Martin, *et al.*, Ensembl 2023. *Nucleic Acids Res.* **51**, D933–D941 (2023).

801 106. Scholz, F, Zhu, A, kSamples: K-Sample Rank Tests and their Combinations. (2023).

802 107. G. Csárdi, T. Nepusz, The igraph software package for complex network research in (2006).

803 108. K. P. Maruska, J. M. Butler, C. Anselmo, G. Tandukar, Distribution of aromatase in the brain
804 of the African cichlid fish *Astatotilapia burtoni* : Aromatase expression, but not estrogen
805 receptors, varies with female reproductive-state. *J. Comp. Neurol.* (2020).

806

Figures and Tables

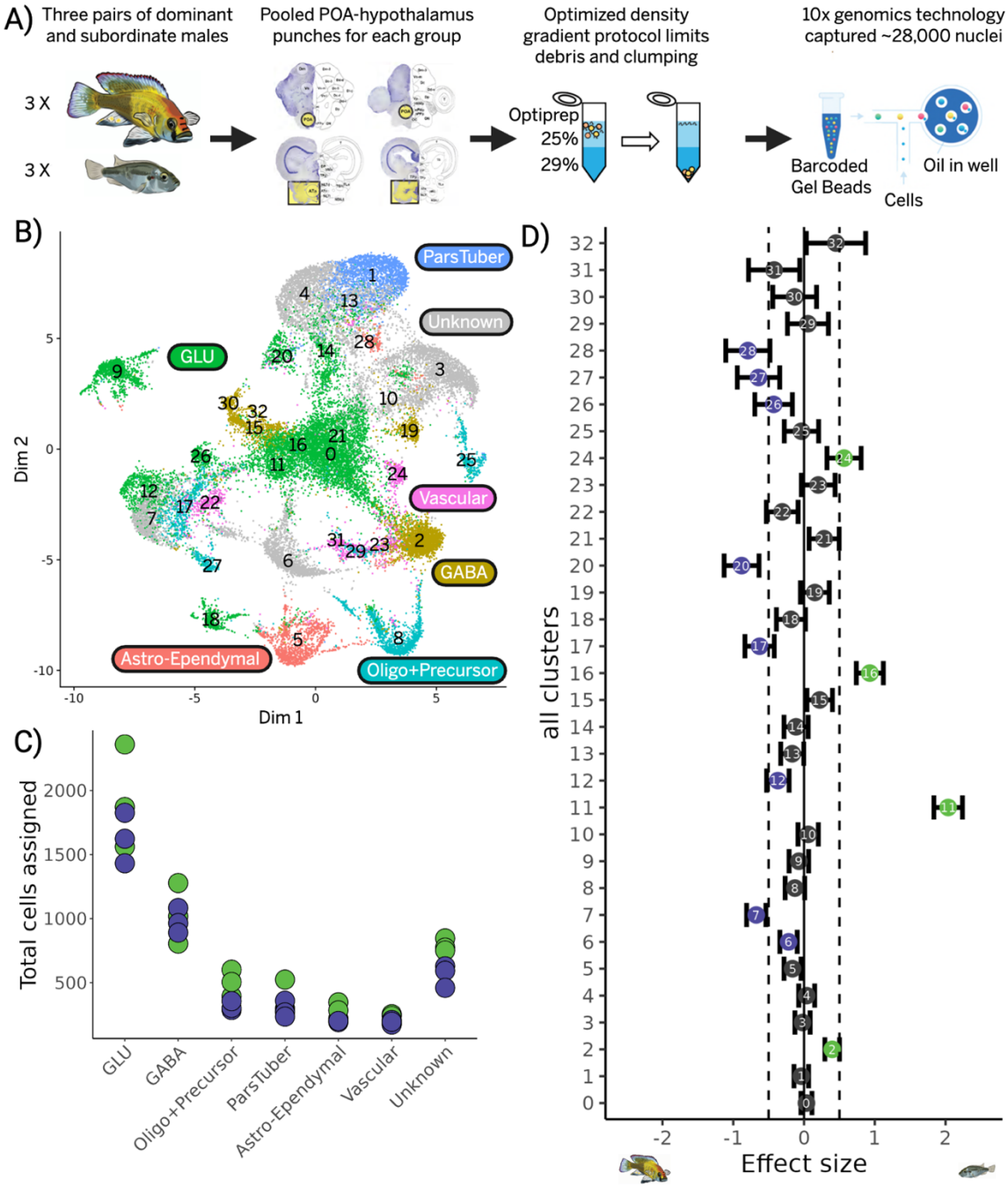

Figure 1. Experimental overview for snRNA-seq pipeline and cell type identification. A) Three pairs of dominant (top) and subordinate male (bottom) *A. burtoni* were collected and the POA-hypothalamus (highlighted in yellow) were pooled for each group prior to single nuclei isolation and snRNA-seq with 10x genomics. Fish illustrations courtesy of Dr. Caitlin Friesen. Brain images from (108). Barcode image courtesy of 10x Genomics. B) UMAP projection of single nuclei data with statistical clusters numbered and cell type assignments color-coded with labels. C) Cell type identification resulted in roughly equal total cells assigned across all genotypes for dominant (purple) and subordinate (green) males. D) Forest plot depicting effect of social status on

817 percentage of nuclei in each cluster and 95% confidence interval with color denoting significant
818 difference (p-value < 0.01) between dominant (purple) and subordinate (green). Dashed lines
819 indicate effect size of 0.5.

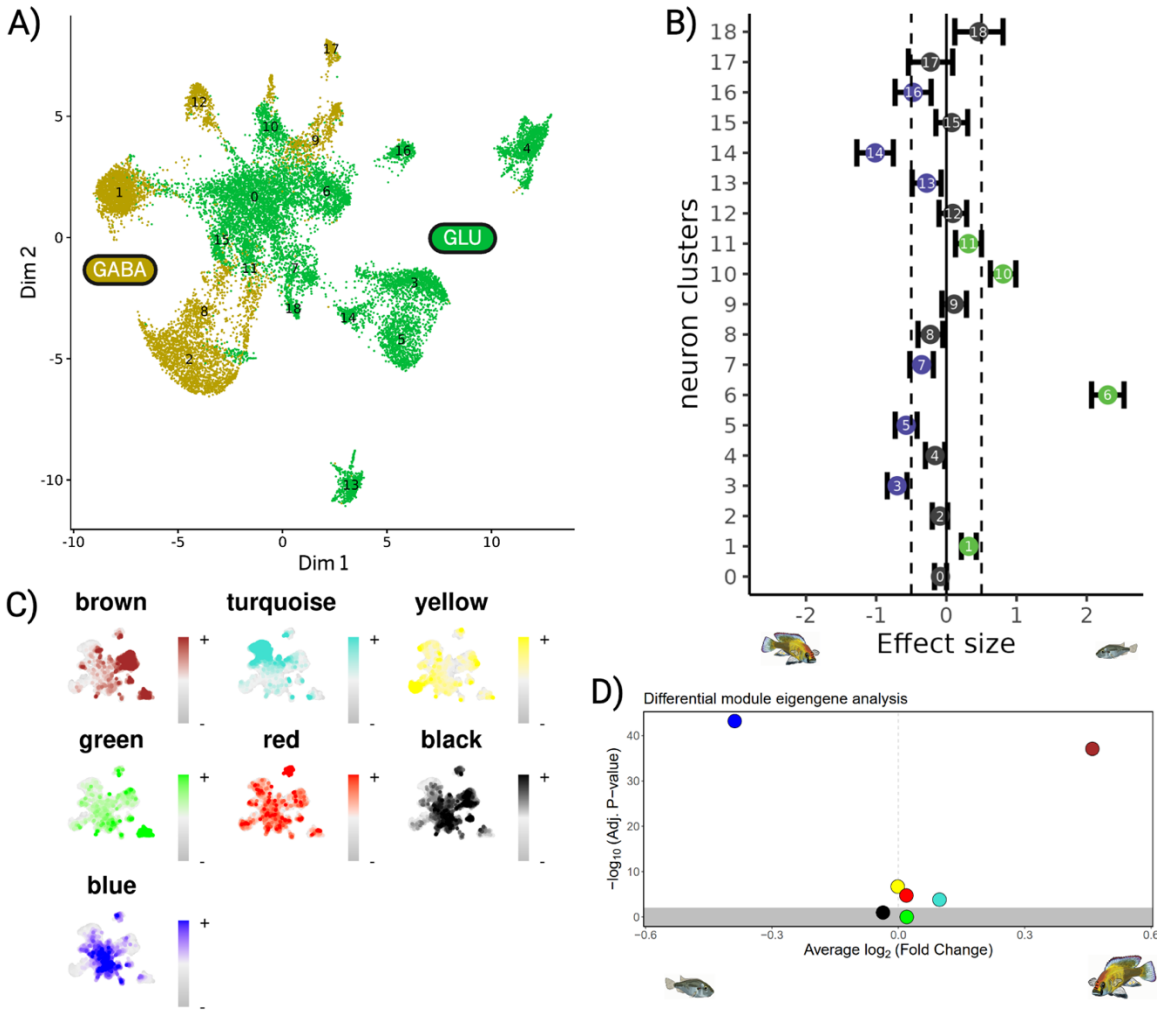

Figure 2. Neuron gene network analysis. A) UMAP projection for all neuron nuclei with statistical clusters numbered and color-coded with labels into excitatory (GLU = green) and inhibitory (GABA = yellow) neurons. B) Forest plot depicting effect of social status on percentage of nuclei in each neuron cluster and 95% confidence interval with color denoting significant difference (p-value < 0.01) between dominant (purple) and subordinate (green). Dashed lines indicate effect size of 0.5. C) Implementation of single-cell optimized weighted gene co-expression network analysis, hdWGCNA, identified six gene expression modules. hdWGCNA module eigengene values across neuronal UMAP space illustrate how most gene co-expression networks are expressed across neurons. D) Gene modules show significant differential expression across social status.

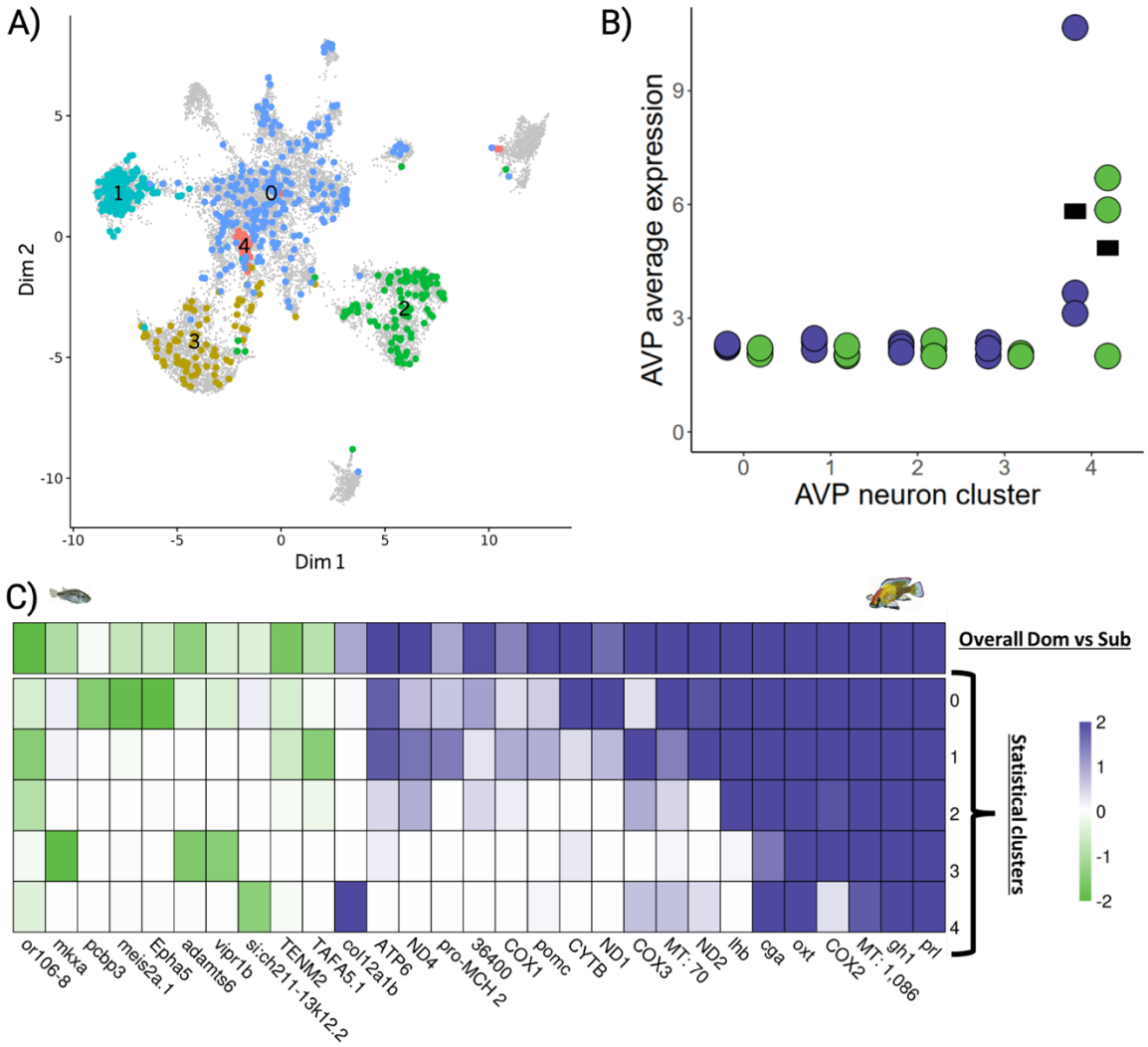

Figure 3. AVP expressing neuron subpopulations. A) Projection on neuron UMAP of all AVP expressing neurons colored and labelled by the five statistical AVP neuron subpopulation clusters. B) Average AVP expression of each AVP neuron statistical clusters for dominant (purple) and subordinate (green) males. C) Heatmap of statistically significant (adjusted p-value < 0.05) DEGs determined by limmatrend analysis across genotypes for all AVP expressing and for each AVP neuron statistical cluster with scale denoting log fold change between dominant bias (purple) and subordinate bias (green).

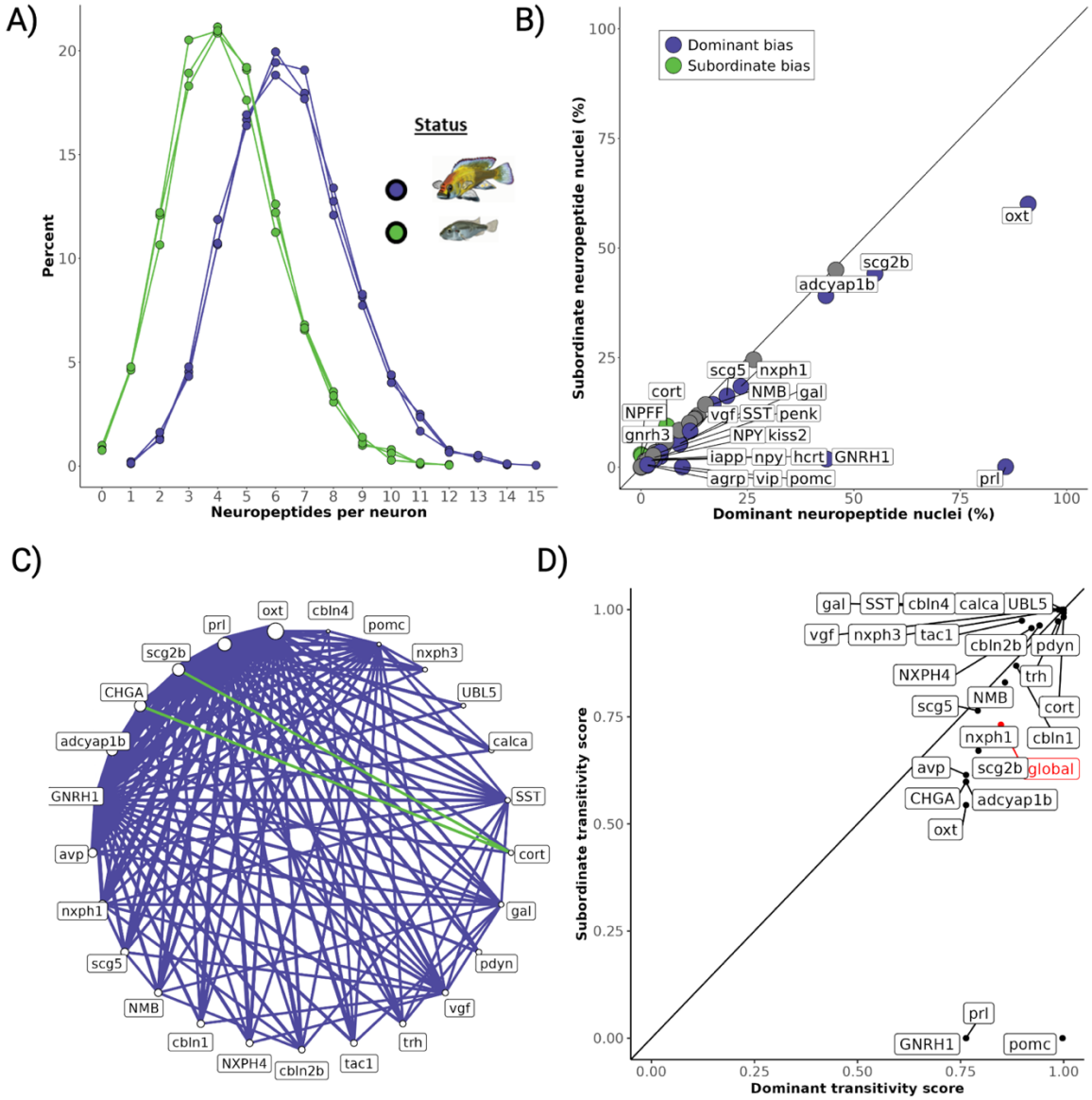

Figure 4. Uncovering the transcriptomic neuropeptidome. A) Neurons broadly express neuropeptide genes, dominant male (purple) neurons have a higher percentage of neuropeptide co-expression than subordinate (green). B) The average percent of neurons expressing each neuropeptide across social status with proportionally significantly different (Binomial GLM FDR p-value < 0.05) neuropeptides colored and labelled for dominate bias (purple) and subordinate bias (green). C) Significantly (FDR p-value < 0.05) different edges between the dominant (purple) and subordinate (green) neuropeptide gene co-expression network. D) Comparison of network clustering through transitivity across social status both overall (global) and locally for each neuropeptide gene, with higher value indicating greater shared connections.